Available online at www.sciencedirect.com
SCIENCE DIRECT®
Journal of Power Sources 144 (2005) 358–364
JOURNAL OF POWER SOURCES
www.elsevier.com/locate/jpowsour

Electrochemical properties of lead dioxides formed on various lead alloy substrates

Masashi Shiota[a,*], Tsuyoshi Kameda[a], Kazumasa Matsui[a], Nobumitsu Hirai[b], Toshihiro Tanaka[b]

[a] *R&D Department, Technical Development Center, GS Yuasa Manufacturing Ltd., 1 Inobanba-cho, Nishinosho, Kisshoin, Minami-ku, Kyoto 601-8520, Japan*
[b] *Department of Materials Science and Processing, Graduate School of Engineering, Osaka University, 2-1 Yamadaoka, Suita 565-0871, Japan*

Available online 30 December 2004

Abstract

Electrochemical properties of lead dioxides, formed on various lead alloy substrates (Pb–In, Pb–Sn, Pb–Sb, Pb–Tl and Pb–Bi), were investigated using electrochemical techniques with X-ray diffraction (XRD) and electron probe micro analyzer (EPMA). Additive elements, selected by applying Hume-Rothery rules, have similar atomic radius and electronegativity to lead. The reduction capacity of lead dioxides that were formed on Pb–Sb and Pb–Sn alloy substrates decreased, whereas the reduction capacity of lead dioxides formed on Pb–In, Pb–Tl and Pb–Bi alloy substrate increased, compared with those formed on the pure lead substrate. The change of the lattice constant of β-lead dioxides and the existence of additive elements in the lead dioxide layer were confirmed from the analysis results of XRD and EPMA. We concluded that the substitution of additive elements for lead in the β-lead dioxide caused the change of its lattice constant to affect the reduction capacity.

Keywords: Lead alloy; Lead dioxide; Lead–acid battery

1. Introduction

The lead–acid battery has many advantages, such as high power density, wide usable temperature range, complete recycling system and low price. For these reasons, the lead–acid battery has been used for numerous purposes. Antimony is responsible for rapid self-discharge and rapid water loss because of reduction of the hydrogen over-potential on lead electrodes. Although the lead–acid batteries had these problems when the lead alloy grid, containing higher Sb contents (Pb-high Sb alloy) was used, these harmful effects on the battery have become less significant since lead alloy grids, containing lower Sb contents (Pb-low Sb alloy) or Pb–Ca–(Sn) alloy grid have been applied [1].

Using such Pb-low Sb alloy or Pb–Ca–(Sn) alloys for the positive grid, however, can make the cycle life performance of the positive plate reduce rapidly, and it has been explained that this phenomenon (premature capacity loss (PCL)) is mostly caused by the formation of a barrier layer at the interface between the positive active material (PAM) and the grid [2,3]. To clarify the effect of antimony, we investigated the characteristics of lead dioxides that were formed on pure lead substrate and Pb–Sb alloy substrate using electrochemical technique, EC-AFM observation, XRD analysis and EPMA analysis [4,5]. Consequently, we reported the antimony effect as follows; the reduction capacity and the particle diameter of the lead dioxides became smaller; the interatomic distance of β-lead dioxide crystal shrank. We suggested from these results that the antimony atoms were doped into the β-lead dioxide crystal structure. We think that the doping of antimony into the β-lead dioxide crystal structure influenced the morphology and the reactivity of the lead dioxides.

This paper focuses on the reactivity of the lead dioxides by additive elements. When we try to add some elements

* Corresponding author. Tel.: +81 75 316 3614; fax: +81 75 316 3091.
E-mail address: masashi.shiota@jp.gs-yuasa.com (M. Shiota).

0378-7753/$ – see front matter © 2004 Elsevier B.V. All rights reserved.
doi:10.1016/j.jpowsour.2004.11.014

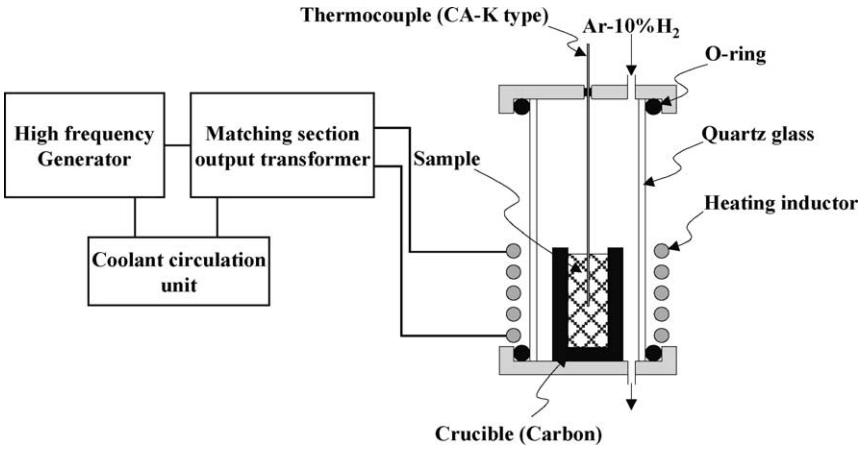

Fig. 1. High frequency induction heating device.

that were easily doped into the lead dioxide crystal structure on the basis of the above antimony effects, there is no index to predict whether the elements can be doped or not. Therefore, we selected some elements according to Hume-Rothery rules [6], which defines the law of solid solutions for a metal. Some parts of Hume-Rothery rules are shown as follows:

(1) Extensive substitutional solid solution occurs only if the relative difference between the atomic diameters (radii) of the two species is less than 15% (Atomic size factor rule).
(2) Electronegativity difference close to 0 gives maximum solubility (Electronegativity rule).

Then, we decided to adopt the indium (In), tin (Sn), antimony (Sb), thallium (Tl) and bismuth (Bi) elements with a difference within 15% compared with the atomic radius of lead atoms [7] (Atomic size factor rule) and within 0.1 compared with the electronegativity of lead atoms [8] (Electronegativity rule) (Table 1) [9,10]. The concentration of additive elements was selected within the range 0.1–3 mass%. In this paper, we have measured the electrochemical properties of lead dioxides which were formed on various lead alloy substrates, containing the above metallic elements and we have investigated the effect of the additive elements on the reactivity of lead dioxides.

Table 1
Atomic radius and electronegativity of elements

Elements	Atomic radius (Å)	Electronegativity
Pb	1.746	1.8
In	1.660	1.7
Sn	1.620	1.8
Sb	1.59	1.9
Tl	1.712	1.8
Bi	1.70	1.9

2. Experimental

2.1. Preparation of lead alloy electrodes

The lead alloys were made by a high frequency induction-heating device (Fig. 1) in an Ar–10% H_2 gas atmosphere to avoid the oxidation of additive elements. The procedure is as follows; the specimen of metals weighed at a given composition was heated to about 100 °C higher than the liquidus line for each alloy and then it was maintained for 10 min and cooled naturally. Next, the lead alloys were melted again at 470 °C by the melting furnace and sample electrodes were made by gravity mold casting at 170 °C. These electrodes' size was 100 mm in length, 20 mm in width and 2 mm in thickness.

2.2. Pretreatment of lead alloy electrode

Fig. 2 shows the procedure for pretreatment of the lead alloy electrode. The electrode surface was polished with abrasive papers and buffed with fine Al_2O_3 powder. Then, the electrode surface was polished chemically with a mixed solution of acetic acid and hydrogen peroxide, and was finally wiped by cloth absorbed with ethanol. After the sample electrode was assembled into the cell, the cell was filled with 1.250 g cm^{-3} sulfuric acid electrolyte. The

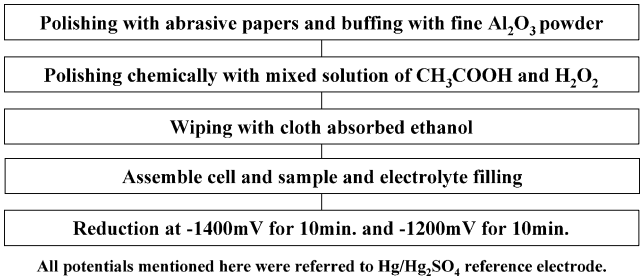

Fig. 2. Procedure of pretreatment of lead alloy electrode.

electrochemical operations were carried out using a potentio/galvano stat (model HZ-3000) made by Hokuto Denko Co. The atmosphere temperature was maintained at 25 °C through the whole experiment. The cell consisted of a PbO_2 electrode as a counter electrode and a Hg/Hg_2SO_4 electrode as a reference electrode. All potentials reported here are referred to this electrode. The electrode was reduced by two steps of potential, starting at −1400 mV for 10 min followed by −1200 mV for 10 min, to remove lead sulfates from the surface.

2.3. Measurement of reduction capacity

The lead dioxides were formed on the electrode surface by applying, 10 times, a potential cycle comprising 1250 mV (oxidation potential) for 10 min and 950 mV (reduction potential) for 30 s. In this paper, the reduction capacity corresponds to the total charge when the potential was changed from 1250 to 950 mV at 10th cycle.

2.4. XRD analysis and EPMA analysis

Test samples were washed with ethanol and dried after oxidation at 1250 mV for more than 2 h. In order to investigate the crystal structure of the formed lead dioxide layer on each alloy substrate, X-ray diffraction (XRD) analysis was performed with a model RINT 2500 V made by Rigaku Co. The Cu Kα radiation (1.54056 Å) was used and the scanning rate was set at $0.5^\circ\,min^{-1}$ with a 2θ range between 20° and 60°. EPMA analysis was performed with a model EPMA-8705 made by Shimadzu Co. to examine the distribution of the additive element in the specimens.

3. Results and discussion

3.1. Reduction capacity

Fig. 3 shows the relation between the amount of additive elements and the reduction capacity of lead dioxides formed on various lead alloy substrates. The reduction capacity has changed approximately in a linear trend with the amount of additive elements. Thus, we obtained the interpolated values of the reduction capacity with 1 atom% addition of each additive by the collinear approximation to compare the effect of the additive elements on the reduction capacity with each other as shown in Table 2. It is found from this table that the reduction capacity of lead dioxides which were formed on Pb–Sb and Pb–Sn alloy substrate has decreased, whereas the reduction capacities of lead dioxides formed on Pb–In, Pb–Tl and Pb–Bi alloy substrate has increased compared with that of pure lead substrate. In the following section, we discuss the main factors to determine the above change in the reduction capacity with different additive elements.

Table 2
Interpolated reduction capacity of lead dioxide with 1 atom% addition of each additive

Elements	Reduction capacity ($\mu Ah\,cm^{-2}$)
Pb	32.3
In	34.5
Sn	31.2
Sb	27.9
Tl	39.5
Bi	41.3

3.2. Microstructure

The grain boundary in a metallic material is recognized to be an unstable interface because it produces easily the segregation and the deposition of compounds. Thus, the grain boundary of lead alloy substrates might control by priority the reduction capacity by changing the amount of lead dioxides. Fig. 4 shows the microstructure of the pure lead and the lead alloys. The single-phase structure was observed in Pb–Sn, Pb–In and Pb–Tl alloys. On the other hand, dendritic structures were found in Pb–Sb and Pb–Bi alloys. The grain size of the lead alloys was smaller than that of the pure lead. However, there was no correlation between the microstructure of the lead alloys and the reduction capacity of lead dioxides.

3.3. XRD result

3.3.1. Ratio of β-lead dioxide to α-lead dioxide

We wonder whether the reduction capacity changes by the difference of the ratio of β-lead dioxide to α-lead dioxide that was formed on each alloy substrate, because the reactivity of β-lead dioxide was higher than that of α-lead dioxide. The ratio of the amount of β-lead dioxide to that of α-lead dioxide was calculated by using the peak intensity of α-lead dioxide (1 1 1) and β-lead dioxide (1 0 1) in XRD (Table 3). Although it is found from Table 3 that the order of the value of β-lead dioxide/α-lead dioxide was Pb–In > Pb–Sn = Pb–Bi > Pb–Tl > pure Pb = Pb–Sb, there was no correlation between the ratio of β-lead dioxide/α-lead dioxide and the reduction capacity of lead dioxides.

3.3.2. Crystal structure of β-lead dioxide

The diffraction angle of β-lead dioxide (1 0 1) and β-lead dioxide (2 1 1) were analyzed in detail for the samples after the electrochemical experiments. The results are shown in

Table 3
Ratio of β-PbO_2 to α-PbO_2

Substrates	β-PbO_2 (1 0 1)/α-PbO_2 (1 1 1)
Pure Pb	1.3
Pb-3 mass% In	2.5
Pb-3 mass% Sn	1.9
Pb-3 mass% Sb	1.3
Pb-3 mass% Tl	1.7
Pb-3 mass% Bi	1.9

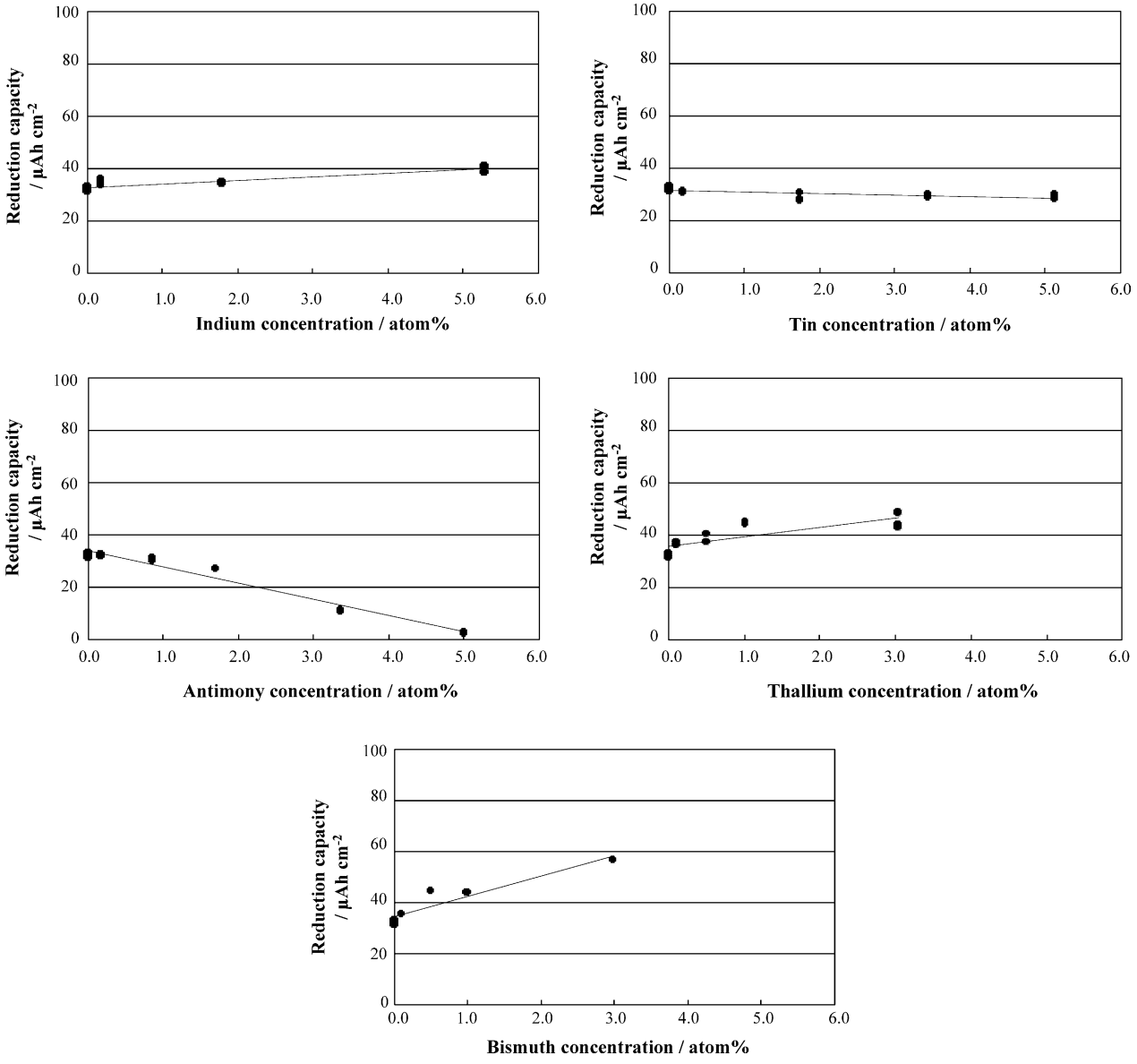

Fig. 3. Reduction capacity of lead dioxide formed on various lead alloy substrates.

Figs. 5 and 6. By comparing the peak of lead, we confirmed that there was no error of the inclination by the setting of the sample (Fig. 5). From the comparison of the diffraction angles of the β-lead dioxide, it was found that the peak on the lead alloy substrates shifted with respect to that on pure lead. Fig. 7 shows the result of the lattice constant of β-lead dioxide that was calculated from the two peaks of β-lead dioxide (1 0 1) and β-lead dioxide (2 1 1). The lattice constant of the *a* and *b* axes has been clearly affected by the additive elements, but the lattice constant of the *c* axis has barely changed. It is noteworthy that the reduction capacity of lead dioxides has decreased when the lattice constant of the *a* and *b* axes has shrunk, compared with that of pure lead substrate, in lead dioxides formed on, such as Pb–Sb and Pb–Sn alloy substrate. On the other hand, the reduction capacity of lead dioxides has increased when the lattice constant of the *a* and *b* axes has elongated in lead dioxides formed on, such as Pb–In, Pb–Tl and Pb–Bi alloy substrates.

3.4. EPMA analysis

We analyzed the distribution of additive elements (Sb, Sn, In, Tl and Bi) in the substrates and the lead dioxides using EPMA. As a result, the segregation of the additive elements was observed in the substrates, and the additive elements were distributed almost uniformly in the lead dioxides (Fig. 8). It has been established that the additive elements exist in the lead dioxide layer.

3.5. Ion radius

From the analysis results of XRD and EPMA, we considered that the change in the lattice constant of β-lead dioxide

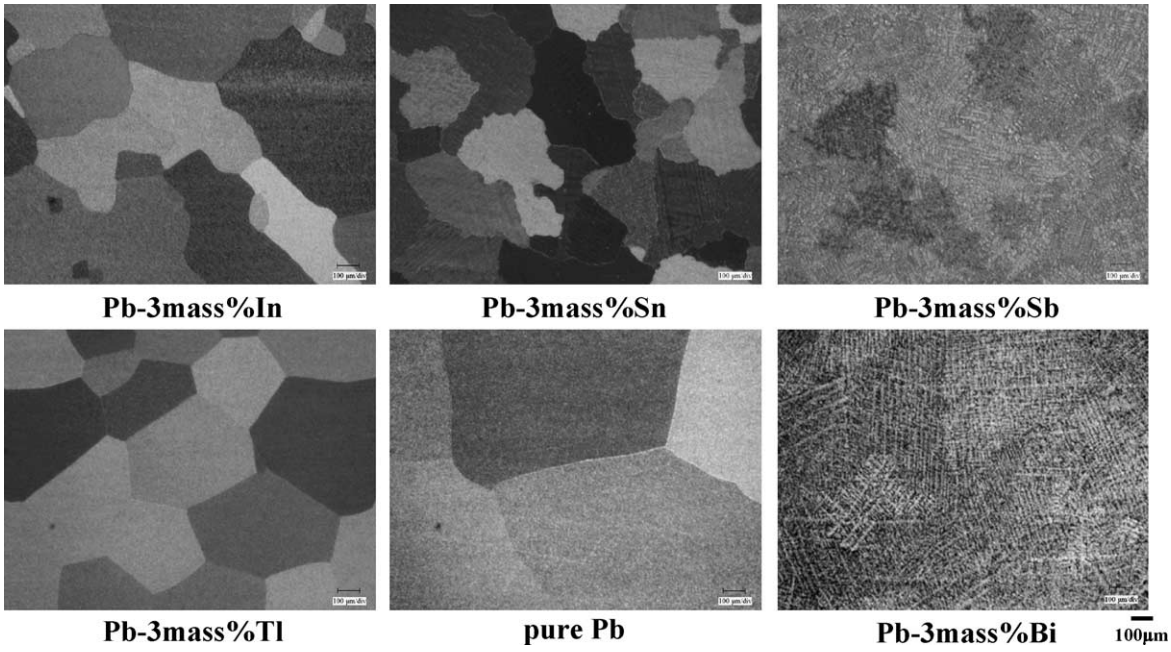

Fig. 4. Microstructure of pure lead and lead alloys.

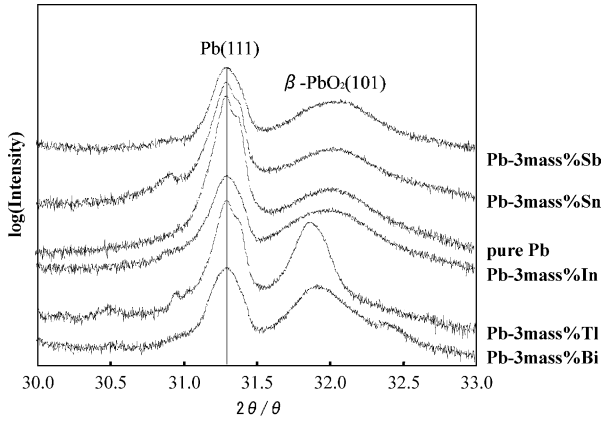

Fig. 5. XRD pattern of β-PbO_2 (1 0 1).

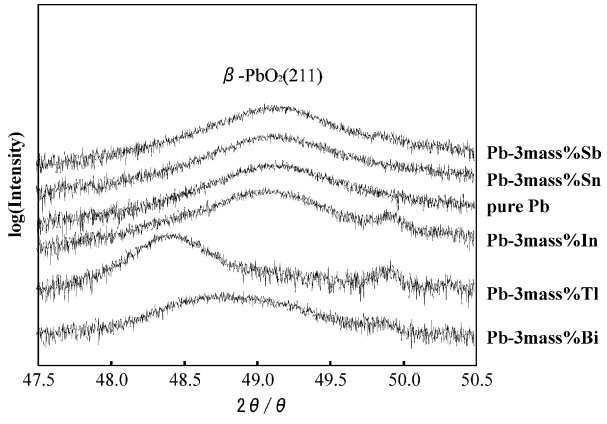

Fig. 6. XRD pattern of β-PbO_2 (2 1 1).

was related to the effect of the additive elements, which substituted for lead in the lead dioxide, on the reduction capacity. Assuming that the additive elements exist in the β-lead dioxide crystals, it is expected that the additive element is in the ionic state rather than the atomic state. By way of example, the reduction capacity of lead dioxides was compared to the ionic radius of the additive elements. Since, the ionic radius varies with the valence of the ion and it's coordination number, the ionic radius was determined using the valence of the stable ion at the positive electrode potential [11] and the coordination number six of lead dioxide [12] (Table 4). Fig. 9 shows the relation between the ionic radius of additive elements and the reduction capacity of lead dioxides. Consequently, we noticed that the reduction capacity of lead dioxides became smaller with the elements (Sn, Sb) with smaller ionic radius than that of Pb^{4+}, whereas the reduction capacity of lead dioxides became larger with the elements (In, Tl, Bi) with larger ionic radius. We consider that this result provides

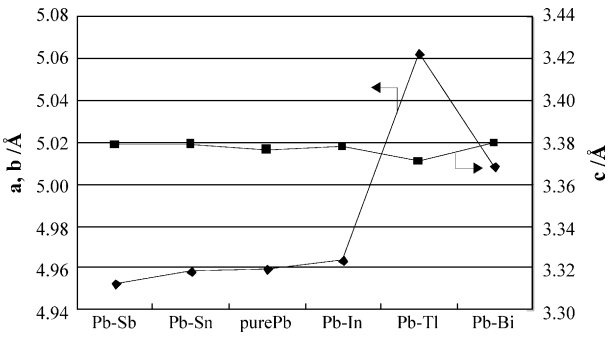

Fig. 7. Lattice constant of β-PbO_2.

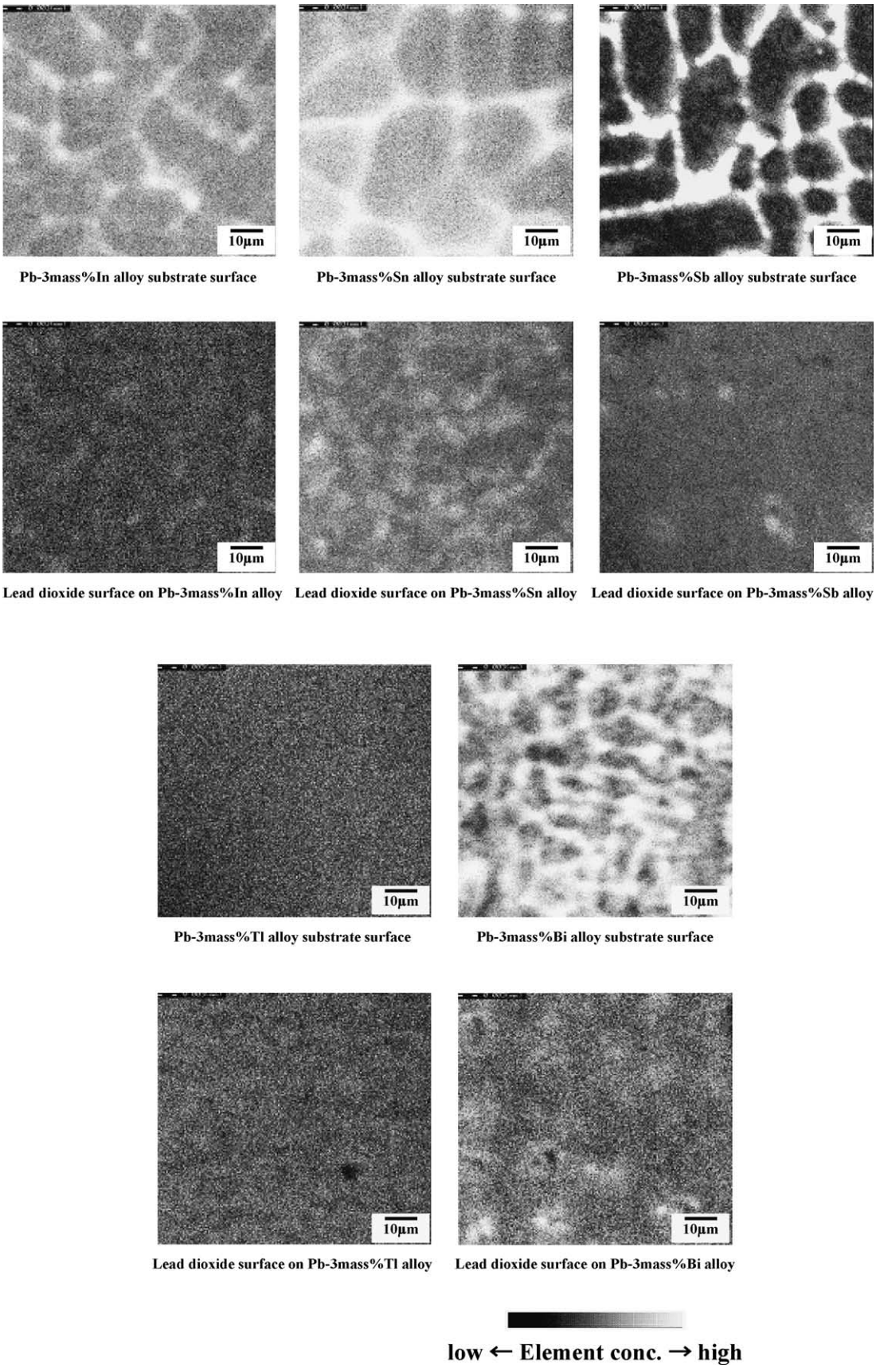

Fig. 8. Distribution of various element in substrate and lead dioxide layer.

Table 4
Ionic radius of element

Elements	Ion	Ionic radius (Å)
Pb	Pb^{4+}	0.775
In	In^{3+}	0.800
Sn	Sn^{4+}	0.690
Sb	Sb^{5+}	0.60
Tl	Tl^{3+}	0.885
Bi	Bi^{3+}	1.03

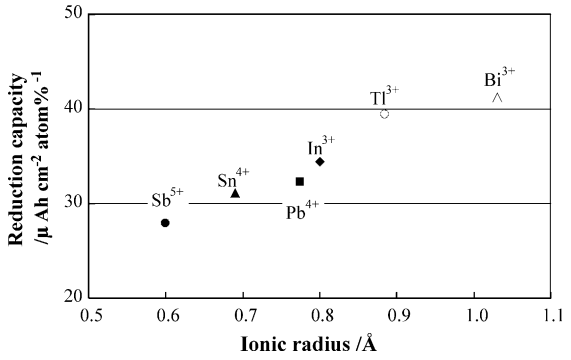

Fig. 9. Relationship between ionic radius and reduction capacity.

additional evidence that the additive elements exist in the lead dioxide crystals.

4. Conclusion

We investigated the electrochemical property of lead dioxides that were formed on various lead alloy substrates (Pb–In, Pb–Sn, Pb–Sb, Pb–Tl and Pb–Bi) using electrochemical techniques, observation of microstructure, XRD and EPMA analysis. The experimental results led to the following conclusions.

1. The reduction capacity of lead dioxides that were formed on Pb–Sb and Pb–Sn alloys substrate has decreased, whereas that formed on Pb–In, Pb–Tl and Pb–Bi alloys substrate has increased compared with the reduction capacity of lead dioxides formed on pure lead substrate.
2. The microstructure of the lead alloy substrates and the ratio of β-lead dioxide/α-lead dioxide were not related to the reduction capacity of lead dioxides.
3. From the results of XRD, the β-lead dioxide lattice constants of the *a* and *b* axes are strongly affected by the additive elements, whereas the *c* axis barely changes.
4. From the analysis results of EPMA, the segregation of the additive elements was observed in the substrates, but the additive elements were distributed almost uniformly in the lead dioxides.
5. We have found Hume-Rothery rules to be useful to select elements, which are capable of substituting for lead in the β-lead dioxide lattice. However, the rules cannot be applied by themselves to predict the effect of doping elements on the reduction capacity of β-lead dioxide.
6. We concluded that the substitution of additive elements for lead in the β-lead dioxides caused the change of their lattice constant and affected their reduction capacity.
7. Substituting ions that are smaller than Pb^{4+} reduces the lattice constant to decrease the reduction capacity of β-lead dioxide, while substituting ions that are larger than Pb^{4+} has the opposite effect.

References

[1] M. Torralba, J. Power Sources 1 (1976–1977) 301.
[2] A.F. Hollenkamp, J. Power Sources 36 (1991) 567.
[3] D. Pavlov, J. Power Sources 42 (1993) 345.
[4] M. Shiota, Y. Yamaguchi, Y. Nakayama, N. Hirai, S. Hara, J. Power Sources 113 (2003) 277.
[5] M. Shiota, Y. Yamaguchi, Y. Nakayama, N. Hirai, S. Hara, YUASA JIHO 94 (2003) 5.
[6] W. Hume-Rothery, G.V. Raynor, The Structure of Metals and Alloys, third ed., The Institute of Metals, London, 1954.
[7] L. Pauling, J. Am. Chem. Soc. 69 (1947) 542.
[8] L. Pauling, The Nature of the Chemical Bond, third ed., Cornell University Press, 1960.
[9] N.E. Bagshaw, J. Power Sources 33 (1991) 3.
[10] N.E. Bagshaw, J. Power Sources 85 (2000) 9.
[11] M. Pourbaix, Atlas of Electrochemical Equilibria in Aqueous Solutions, Pergamon Press, 1966.
[12] R.D. Shannon, Acta Cryst. A32 (1976) 751.